Journal of Chromatography A 1626 (2020) 461361

Contents lists available at ScienceDirect

Journal of Chromatography A

journal homepage: www.elsevier.com/locate/chroma

Chiral determination of nornicotine, anatabine and anabasine in tobacco by achiral gas chromatography with (*1S*)-(-)-camphanic chloride derivatization: Application to enantiomeric profiling of cultivars and curing processes

Kai Cai[a,b], Huina Zhao[a], Runsheng Yin[c], Yechun Lin[a], Bo Lei[a], Anping Wang[d], Wenjie Pan[a], Bin Cai[e], Weichang Gao[a,*], Feng Wang[a,*]

[a] Guizhou Academy of Tobacco Science, Guiyang 550081, China
[b] College of Resources and Environment, Southwest University, Chongqing 400715, China
[c] State Key Laboratory of Ore Deposit Geochemistry, Institute of Geochemistry, Chinese Academy of Sciences, Guiyang 55081, China
[d] Key Laboratory for Information System of Mountainous Area and Protection of Ecological, Environment of Guizhou Province, Guizhou Normal University, Guiyang, Guizhou 550025, China
[e] Haikou Cigar Research Institute, Hainan Provincial Branch of China National Tobacco Corporation, Haikou 571100, China

ARTICLE INFO

Article history:
Received 25 March 2020
Revised 1 June 2020
Accepted 19 June 2020
Available online 20 June 2020

Keywords:
Tobacco
Alkaloids
Chiral derivatization
Validation
Cultivars
Curing processes

ABSTRACT

The alkaloid enantiomers are well-known to have different physiological and pharmacological effects, and to play an important role in enantioselectivity metabolism with enzymes catalysis in tobacco plants. Here, we developed an improved method for simultaneous and high-precision determination of the individual enantiomers of nornicotine, anatabine and anabasine in four tobacco matrices, based on an achiral gas chromatography-nitrogen phosphorus detector (GC–NPD) with commonly available Rtx-200 column using (*1S*)-(-)-camphanic chloride derivatization. The method development consists of the optimization of extraction and derivatization, screening of achiral column, analysis of the fragmentation mechanisms and evaluation of matrix effect (ME). Under the optimized experimental conditions, the current method exhibited excellent detection capability for the alkaloid enantiomers, with coefficients of determination (R^2) > 0.9989 and normality test of residuals $P > 0.05$ in linear regression parameters. The ME can be neglected for the camphanic derivatives. The limit of detection (LOD) and limit of quantitation (LOQ) ranged from 0.087 to 0.24 $\mu g\ g^{-1}$ and 0.29 to 0.81 $\mu g\ g^{-1}$, respectively. The recoveries and within-laboratory relative standard deviations (RSD_R) were 94.3%~104.2% and 0.51%~3.89%, respectively. The developed method was successfully applied to determine the enantiomeric profiling of cultivars and curing processes. Tobacco cultivars had a significant impact on the nornicotine, anatabine, anabasine concentration and enantiomeric fraction (EF) of (*R*)-nornicotine, whereas the only significant change induced by the curing processes was an increase in the EF of (*R*)-anabasine.

1. Introduction

Tobacco contains mainly nicotine and minor structurally related alkaloids which consist of nornicotine, anatabine, and anabasine [1]. During the curing and processing of tobacco, the nitrosation of the secondary amine groups of nornicotine, anatabine and anabasine under mild conditions produces nitrosonornicotine (NNN), nitrosoanatabine (NAT) and nitrosoanabasine (NAB), respectively. These three minor alkaloids have been recognized as the primary precursors of the highly carcinogenic tobacco-specific nitrosoamines [2]. They are present as pairs of enantiomers due to the chiral center at the 2′-C position on their pyrrolidine or piperidine ring. The enantiomers are well-known to have different pharmacological effects and physiological activities [3]. Moreover, the metabolic pathway of alkaloids in tobacco is also enantioselective due to the selectivity of the enzymes involved [4]. Overall, enantiomeric analysis of nornicotine, anatabine, and anabasine will not only benefit pharmacological studies, but also lead to a better understanding of the metabolic fates of the chiral alkaloids in tobacco.

* Corresponding authors.
E-mail addresses: gzyksg@163.com (W. Gao), yancaowangfeng@163.com (F. Wang).

https://doi.org/10.1016/j.chroma.2020.461361
0021-9673/

Currently, a relatively large number of previous studies have reported for qualitative and quantitative analysis of tobacco alkaloids with gas chromatography (GC) or liquid chromatography (LC) [5–7]. However, chiral separation and quantification of alkaloid enantiomers were less reported. The available chiral separation techniques mainly include chiral stationary phases, chiral selectors in the mobile phase or chiral derivatization reagents [8–10]. Analytical columns with chiral stationary phases (such as crosslinked cyclodextrins, polysaccharides and protein) can be employed with either LC or GC. Trifluoroacetylation as a derivatization approach followed with gas chromatography-mass spectrometry (GC–MS) or multi-dimensional GC–MS chiral analysis with crosslinked cyclodextrins was applied for separation of the enantiomers of nornicotine, anatabine, and anabasine in tobacco, however, the enantiomers were not completely separated without the MS selected ion mode and strict quantitative data were not obtained [11,12]. Recently, ultra-performance liquid chromatography-tandem mass spectrometry using chiral acid glycoprotein and cellulose-2 column was applied to determine alkaloid enantiomers in tobacco. This method is simple, fast and sensitive for the complete separation. However, some shortcomings such as a relatively high matrix effect (ME) and poor column stability were observed [13]. Moreover, chiral columns are often expensive compared to reverse-phase columns and may require extensive development time and cost [14]. Chiral selectors are often used as additives for chiral separation in LC or capillary electrophoresis (CE). Kodama and coworkers reported the simultaneous enantioseparation of alkaloid enantiomers in tobacco by CE using sulfated β-cyclodextrin as a chiral selector [15]. This method required two or three sequential solid-phase extraction pretreatments and provided relatively low sensitivity. Furthermore, chiral selectors may easily cause instrumental contamination and reduce the method stability and column lifetime [16]. Chiral derivatization reagents are chiral auxiliaries used to convert a mixture of enantiomers into diastereomers, which can be separated with achiral GC or LC. Although chiral derivatization may slightly increase the sample preparation time, the analytes can be separated with low ME, excellent peak shape and without requiring a special mobile phase or chiral column. Additionally, many chiral derivatization reagents are inexpensive and easily available [17].

The Schotten–Baumann reaction with biphasic derivatization mechanism was adopted for chiral derivatization of the alkaloids. Primary and secondary amines alkaloids can be acylated by an (*1S*)-(-)-camphanic chloride under alkaline aqueous conditions [18]. This reaction is simple, fast, and quantitative, and provides stable reaction products that are easily separated using achiral chromatography. In addition, this reagent is cost-effective [19]. (*1S*)-(-)-camphanic chloride has been proven as an efficient chiral derivatization reagent for determination of the nornicotine enantiomers with achiral GC, but complex pretreatment of thin layer chromatography were used and chiral separation was limited to nornicotine enantiomer [20,21]. Overall, (*1S*)-(-)-camphanic chloride derivatization combining with achiral GC for baseline separation of the enantiomers of nornicotine, anatabine, and anabasine has not been well established.

In this study, we developed an improved method for the simultaneous determination of the enantiomers of nornicotine, anatabine, and anabasine in four tobacco matrices application of chiral derivatization and achiral GC. The procedures involved extraction with alkaline dichloromethane, without further purification, derivatization with (*1S*)-(-)-camphanic chloride and baseline separation (R_s>1.5) of the camphanic derivatives with conventional gas chromatography-nitrogen phosphorus detector (GC–NPD) using an Rtx-200 achiral column with a trifluoropropyl stationary phase. The method development consisted of the optimization of extraction and derivatization, screening of achiral column, analysis of the fragmentation mechanisms and evaluation of ME. The Box–Behnken design (BBD) was applied to optimize the camphanic derivatization conditions and then the method validation was performed with linearity, ME, sensitivity, recovery, precision and stability using the optimum conditions. Finally, the variations in the alkaloid concentration and enantiomer fraction (EF) of flue-cured tobacco (FCT) from different cultivars and curing processes were investigated.

2. Experimental design

2.1. Chemicals and reagents

All chemicals were of analytical grade unless otherwise indicated. The racemic (*R/ S*)-nornicotine, (*R/S*)-anatabine and (*R/S*)-anabasine (≥98%) and the optically pure enantiomers (*S*)-nornicotine, (*R*)-anatabine, and (*S*)-anabasine (≥98%) were purchased from TRC (Toronto Research Chemicals Inc., Canada). The derivatization reagent of (*1S*)-(-)-camphanic chloride (≥97%), the internal standard (IS) of 4-phenylpiperidine (≥98%) and the surrogate of 4-phenylpyridine were procured from TCI (Tokyo, Japan). Dichloromethane, sodium hydroxide, methyl tert–butyl ether, methanol, hexane and other reagents were procured from Sinopharm Chemical Reagent (Beijing, PRC). Ultrapure water was prepared using a Milli-Q system (Millipore, Bedford, MA, USA).

2.2. Preparation of standard solutions and samples

The 4-phenylpiperidine (5.4 mg mL^{-1}), 4-phenylpyridine (1.0 mg mL^{-1}), standard stock solutions of (*R/S*)-nornicotine, (*R/S*)-anatabine and (*R/ S*)-anabasine with concentration of 1.0 mg mL^{-1} and the optically pure analytes of (*S*)-nornicotine, (*R*)-anatabine and (*S*)-anabasine with concentration of 1.0 mg mL^{-1} were prepared in dichloromethane and stored at 4 °C. A series of mixed calibration standard solutions with six concentrations of (*R/S*)-nornicotine and (*R/S*)-anatabine of 0.4, 1.0, 5, 20, 50, 200 μg mL^{-1}, (*R/S*)-anabasine of 0.1, 0.5, 2.5, 5, 25, 50 μg mL^{-1} were freshly prepared before use by diluting the standard stock solution with dichloromethane. The (*1S*)-(-)-camphanic chloride and NaOH solutions were prepared by dissolving these reagents in dichloromethane and ultrapure water, respectively, to obtain the desired concentration.

The four tobacco matrices of FCT, burley tobacco (BT), oriental tobacco (OT) and freeze-dried fresh flue-cured tobacco (FD-FFCT) were used for method validation. The FCT (cultivar and leaf grade: Yunyan 87 and C3F) was a standard reference sample, gifted by the Yunnan Academy of Tobacco Agricultural Sciences and used for optimization of experimental conditions. The concentration of nornicotine (764.8 ± 12.5 μg g^{-1}), anatabine (1285.6 ± 13.7 μg g^{-1}) and anabasine (130.6 ± 3.7 μg g^{-1}) in the standard reference sample were certified by three laboratories using the same standard method (YC/T 559–2018). This method involves alkalization with a 5% NaOH solution, dichloromethane/methanol (4:1 *v/v*) extraction, and GC–MS determination. To investigate the enantiomeric profiling of alkaloids in FCT cultivars and curing processes, seven cultivars with different nicotine synthesis levels (NC297, Bina 1, K326, Corker17, NC82, NCTG55 and NC95, leaf position from bottom to top: 11th leaf) were selected. As Bina 1 and K326 have a large planting area in Guizhou province, China, FD-FFCT was further prepared to study the influence of the curing processes. The seven cultivars were grown at research plots at a tobacco planting base in Fuquan city, Guizhou province. The field design was a complete randomized block with each cultivar. Seedlings were grown in a greenhouse, transplanted to the field on April 25, 2018, and subsequently grown according to standard tobacco cultivation protocols for Guizhou province. Tobacco fertilization for base dressing

Table 1
BBD with coded variables, real variables, RRF and model coefficient for ANOVA.

No	Coded variables			Real variables			RRF		
	A	B	C	A/mg mL^{-1}	B/%	C/min	Nornicotine	Anatabine	Anabasine
1	−1	1	0	50	25	25	0.624	0.810	0.0675
2	0	0	0	100	15	25	0.831	1.089	0.1206
3	0	−1	1	100	5	40	0.720	0.918	0.0846
4	−1	−1	0	50	5	25	0.568	0.729	0.0531
5	1	1	0	150	25	25	0.814	1.062	0.1161
6	0	0	0	100	15	25	0.813	1.062	0.1170
7	0	1	−1	100	25	10	0.690	0.882	0.0945
8	0	0	0	100	15	25	0.823	1.044	0.1161
9	1	0	−1	150	15	10	0.695	0.891	0.0801
10	0	−1	−1	100	5	10	0.677	0.864	0.0765
11	0	1	1	100	25	40	0.835	1.107	0.1242
12	0	0	0	100	15	25	0.838	1.134	0.1152
13	1	0	1	150	15	40	0.824	1.098	0.1188
14	0	0	0	100	15	25	0.807	1.116	0.1215
15	1	−1	0	150	5	25	0.716	0.918	0.0864
16	−1	0	1	50	15	40	0.658	0.855	0.0729
17	−1	0	−1	50	15	10	0.594	0.765	0.0594
ANOVA	Model *p*-value						<0.0001	<0.0001	<0.0001
	Lack of fit						0.3619	0.9071	0.1390
	Coefficient of variation						1.88	3.10	4.14
	R^2						0.9901	0.9784	0.9886

(N: P_2O_5: K_2O=10: 10: 25) and top dressing (N: P_2O_5: K_2O=10: 0: 30) was applied with 675 kg hm^{-2} and 225 kg hm^{-2}, respectively. The mature leaves were later harvested and cured in a barn with circulating heated air. To collect the samples of the curing processes, the fresh mature leaves were divided into two parts along the midvein by the half-leaf method. One part was immediately placed in liquid nitrogen, transported to the laboratory, and dried in a vacuum freeze dryer (SIM Inc, DE, USA) to obtain FD-FFCT. The remaining part with the midvein was cured in a barn with circulating heated air. Eight leaves were mixed into each sample and six replications were taken. The FCT samples were oven-dried (55 °C), and ground into 40–60 mesh powder for alkaloid and *R/S* enantiomer analysis. The FD-FFCT samples were also ground into 40–60 mesh powder for analysis.

2.3. Extraction and derivatization procedures

About 200 ± 1.0 mg sample of the FCT, BT or OT tobacco products or 100 ± 0.5 mg sample of the FD-FFCT tobacco products was weighed into a 50 ml screw-cap centrifuge tube. A 50 μL aliquot of 5.4 mg mL^{-1} 4-phenylpiperidine and 1.0 mL of 5% (*w/w*) sodium hydroxide (2.0 mL for FD-FFCT) were added in sequence. After shaking the tube in a Vortex 1 mixer (IKA, Staufen, Germany) for 1 min, 3 mL of dichloromethane was added to the extraction and then the centrifuge tube was capped tightly. The sample was extracted using strong vortex extraction (2500 rpm) with a multi-tube vortex oscillator (TROEMNER, NJ, USA) for 30 min and then centrifuged at 4000 rpm for 5 min. The subnatant was filtered through a 0.45 μm nylon membrane and 0.4 ml of the dichloromethane was transferred into a 2.0 ml centrifuge tube for derivatization.

A 200 μL aliquot of 127 mg mL^{-1} (*1S*)-(-)-camphanic chloride was added and thoroughly mixed. Then, 100 μL of a 21% (*w/w*) NaOH solution was added as an alkaline catalyst, and the tube was capped tightly. The alkaloids were derivatized with vortexing (2500 rpm) for 39 min. After derivatization, a 300 μL aliquot of the subnatant was transferred into a 1.5 mL centrifuge tube and then the surrogate (30 μL with concentration 1 mg mL^{-1}) was added. The mixture solution was evaporated to dryness under nitrogen stream at room temperature. Finally, the resulting residues were dissolved in 100 μL methyl tert–butyl ether and transferred to a 100 μL polypropylene insert with polymer feet in a 2 mL septum vial and analyzed using auto-GC–NPD.

2.4. Optimization of the derivatization with response surface methodology

A multivariate strategy based on the response surface methodology with a three-factor-three-level BBD was employed to optimize derivatization conditions of (*1S*)-(-)-camphanic chloride concentration (mg mL^{-1}) (A), NaOH mass fraction (*w/w*) (B) and reaction time (min) (C). The optimization was performed using 400 μL of extract solution from the FCT standard reference sample and then 200 μL of (*1S*)-(-)-camphanic chloride combined with 100 μL of NaOH solutions were added for derivatization with room temperature vortexing. The coded variables, real variables, relative response factors (RRF) are presented in **Table 1**. The code variables were set as −1, 0, +1 and correspond with the real variables of the A (-1 = 50, 0 = 100, +1 = 150 mg mL^{-1}), B (-1 = 5, 0 = 15, +1 = 25%) and C (-1 = 10, 0 = 25, +1 = 40 min). Since (*1S*)-(-)-camphanic chloride had the same reaction rate with the (*R/S*)-enantiomers under different derivatization conditions, the RRF value was used as indicator for optimization of the total derivatization efficiency (both *R* and *S* enantiomers). The RRF for each analyte was calculated by dividing the peak area of the analyte by surrogate.

2.5. Chromatographic analysis

2.5.1. Column screening

Nine achiral columns with different stationary phases (0%, 5%, 35% or 50% diphenyl/100%, 95%, 65% or 50% dimethylpolysiloxane, 35% trifluoropropyl methylpolysiloxane, 14% cyanopropylphenyl/86% dimethylpolysiloxane and 100% polyethylene glycol), polarities (nonpolarity, midpolarity and polarity) and specification (60 or 30 *m* × 0.32 or 0.25 mm i.d. × 0.25 or 0.5 μm *df*), which are available in most laboratories, were evaluated with the same as those below chromatographic conditions. The racemic standards (*R/S*)-nornicotine, (*R/S*)-anatabine and (*R/S*)-anabasine with concentrations of 1.5, 2.0 and 1.5 μg mL^{-1}, which were prepared by diluting the standard stock solution with dichloromethane, respectively, were used for analysis. The separation capacity was evaluated using the resolution (R_s), which was calculated using the following

formulas: R_s=2(t_2-t_1)/(w_1+w_2), where t is the retention time and w is the width of the peak at the baseline. R_s values greater than 1.50 indicate that baseline separation was achieved.

2.5.2. Chromatographic conditions

GC analysis of the enantiomers of nornicotine, anatabine, and anabasine was performed on a Trace GC-ULTRA gas chromatograph with an AS3000 auto-sampler coupled to an NPD (Thermo Scientific, FL, USA). Helium (99.999% purity) was used as the carrier gas with a flow rate of 1.0 mL min^{-1} in constant flow mode. GC separation with best resolution (R_s>1.5) was performed using an Rtx-200 (60 *m* × 0.25 mm i.d. × 0.5 μm *df* of 35% trifluoropropylmethylpolysiloxane). The temperature of the GC was initially held at 60 °C for 1 min, then increased to 230 °C using a linear gradient of 15 °C min^{-1} and held for 3 min. The temperature was then ramped to 280 °C at 5 °C min^{-1} and held for 13 min, resulting in a total run time of 60.33 min. The temperatures of the injector and detector were 270 °C and 280 °C, respectively. Splitless injection mode (1 μL) was selected. The flow of dry air for the detector was 60 mL min^{-1}, the flow rate of hydrogen (99.999%) was 2.3 mL min^{-1} and the makeup gas helium was 15 mL min^{-1}. The hydrogen delay was 15 min.

2.6. Mass spectrometric analysis

The GC–MS with electron ionization (EI) analysis was carried out on with a Trace GC-ULTRA-ITQ 900 (Thermo Scientific, FL, USA) with an AS3000 auto-sampler. The chromatographic conditions were the same as those above. The ionization voltage was 70 eV. The source and transfer line temperature were kept at 230 °C and 280 °C, respectively. The rate of micro-scanning was 3 scan s^{-1} and the samples were run in full scan mode with a mass range of 50–650 Dalton (atomic mass unit). The enantiomers of nornicotine, anatabine and anabasine were identified using their retention times and mass spectrums. Additionally, the EI-MS fragment of camphanic derivatives were analyzed to obtain fragmentation mechanism.

2.7. Method validation

2.7.1. Linearity, matrix effects, and limits of detection and quantitation

Racemic calibration solutions were prepared in duplicate at six concentrations using the solvent (dichloromethane) and matrix extract solutions (FCT, BT, OT and FD-FFCT). The solvent matched and matrix matched-calibration curves were constructed using weighted (1/X) least-squares linear regression models, by plotting the peak area ratio (y) using the internal standard (10 μL with concentration 5.4 mg mL^{-1}) versus gradient concentration ratio (x). Linearity was evaluated using the coefficient of determination (R^2). The regression models were further evaluated using a D'Agostino-Pearson omnibus K^2 normality test of residuals [22]. To evaluate the ME, the ratios of the slopes for the curves with different matrices with the classical standard addition method were compared using Eq. (1). Positive or negative values of ME were considered to correspond to matrix enhancement or suppression, respectively [23]. Generally, the R^2 should be higher than 0,990 and the ME should be within ± 20% with weak effect on the quantitative analytical results [24].

$$\mathrm{ME}(\%)\left(\frac{\text{Slop of matrix matched curve}}{\text{Slop of solvent matched curve}}-1\right)\times 100 \qquad (1)$$

The LODs and LOQs (in μg g^{-1}) were calculated as 3 and 10 times the signal-to-noise ratio of the lowest solvent matched-calibration standard solution (taking into account derivatization and purification procedure), based on the sample weight, dilution ratio of the sample and recoveries of the target analytes [25].

2.7.2. Recovery, precision and storage stability

Recovery (%) was evaluated with six replicate samples spiked with low- or high-level of the analytes in each matrix. Each of the racemates was spiked, incubated overnight at 4 °C and then extracted. The recovery percentage was calculated using the following equation: R%={[(Concentration of the spiked sample - Concentration of the unspiked sample)/Spiked concentration] × 100}. The acceptance criteria for recovery was between 80% and 120%. The accuracy was further evaluated by comparing alkaloid concentration of standard reference sample. No significant difference indicates high accuracy. The precision was expressed as the within-laboratory (indicated by subscript R) relative standard deviation (RSD_R) and Horwitz ratio (HorRat) [26], which was calculated by analyzing six independent samples on three consecutive days. The HorRat was calculated as the ratio between the experimental and the predicted RSD_R. HorRat values between 0.3 and 1 indicate that the precision of the method in terms of reproducibility is fully acceptable. When the HorRat value is less than 0.3, the method precision may also be acceptable, but a reasonable explanation is required [27]. The storage stabilities of camphanic derivatives with each of the matrices were tested by calculating the relative differences (RDs) between the concentration of the analyte at t = 0 and that at the end of the storage period (t = 7 d) [28]. The RDs were calculated using following equation: RDs={[(Concentration at t = 0 - Concentration at t = 7)/ concentration at t = 0] × 100}. The RDs less than 5% indicate good stability.

2.8. Statistical analysis

The ratio of an individual enantiomer was expressed as the enantiomer fraction (EF), which was calculated as EF = (*R*)-enantiomer/((*R*)-enantiomer + (*S*)-enantiomer)), where (*R/S*)-enantiomer is the peak area or concentration of the R or S form. The extraction efficiency was evaluated with extraction recovery. The analysis of variance (ANOVA) of BBD was conducted using the Design-Expert version 8.0.6 software (Stat-Ease Inc., Minneapolis, MN, USA). The ANOVA for the response surface quadratic model was used to justify the adequacy. This model was used to predict the response at any point, even those not included in the design. To measure how well the proposed model fit the experimental data, the parameters such as model *p*-value, lack of fit, coefficient of variation and R^2, were used. The model *p*-value and coefficient of variation (CV) less than 0.05 and 10, lack of fit and R^2 greater than 0.05 and 0.90 showed a reliable model was obtained. The Student's *t*-test and ANOVA with Fisher's least significant difference (LSD) test were applied for statistical comparison of concentration and EF change using SPSS 16.0 software (SPSS Inc., Chicago, IL, USA). Differences were considered significant when p < 0.05. All diagrams were drawn using Origin 8.0 Software (Origin Lab Corp., USA) and ChemBioDraw Ultra 7.0 (Cambridgesoft.com, MA, USA). Normality testing of the linear regression equations (α=0.05) for evaluation of the regression residuals was performed using GraphPad Prism 7 (GraphPad Software, Inc., USA).

3. Results and discussion

3.1. Optimization of the extraction procedure

The previous study showed that the best results for the extraction efficiency were obtained under the following conditions. This extraction conditions included the alkalization with a 5% NaOH solution and then dichloromethane/methanol (4:1 *v/v*) extraction with oscillation [1]. In this work, the reference stan-

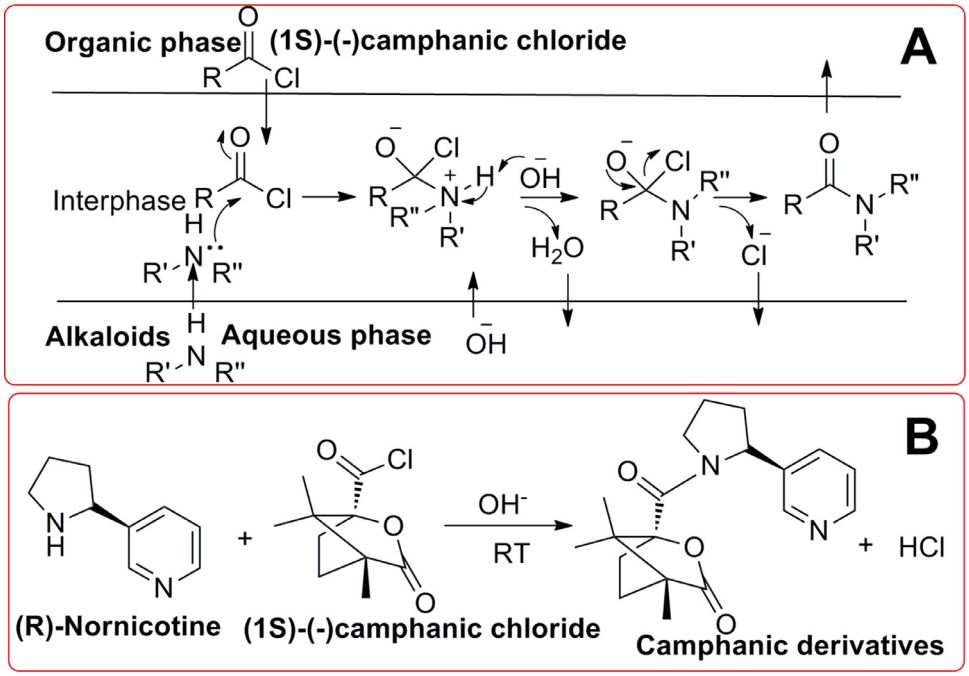

Fig. 1. Biphasic derivatization mechanism for Schotten–Baumann reaction of alkaloids **(A)**, and scheme of the reaction of (*1S*)-(-)-camphanic chloride with (*R*)-nornicotine **(B)**.

dard FCT has been used for the determination of the extraction efficiency. Six replicate samples with each extraction conditions were conducted to evaluate the extraction efficiency with recovery experiment. Because (1S)-(-)-camphanic chloride can react with methanol, dichloromethane was used for extraction instead of a dichloromethane/methanol mixture. Although dichloromethane was reported to have a relatively weak ability to extract alkaloids [29], special attention has been paid to strong vortexing of the sample with a multi-tube vortex oscillator resulting in an extraction efficiency of 96.1~97.8% for nornicotine, 97.6~99.5% for anatabine and 98.4~101.3% for anabasine. These percentages correspond to the results mentioned in previous study [1] and respond to pre-established criteria of 80% to 120% recovery.

3.2. Optimization of derivatization procedure

The biphasic derivatization mechanism for Schotten–Baumann reaction and a scheme of the reaction of (*1S*)-(-)-camphanic chloride with (*R*)-nornicotine are given in Fig. 1. A number of experimental parameters can affect the Schotten–Baumann reaction, including the type of organic phase, reaction conditions, (*1S*)-(-)-camphanic chloride concentration, NaOH mass fraction, and reaction time. Dichloromethane is a useful solvent in a number of biphasic reactions, as it can improve the reactivity of nucleophiles and the extraction capacity towards the derivative products [30]. Moreover, dichloromethane was also used as the extraction solvent, and no extra drying step was required prior to derivatization. Reaction conditions were carried under i.e., room-temperature vortexing, room-temperature ultrasonication, heating in a 40 °C waterbath, and cooling in an ice bath. As detailed in Table 1**S**, room temperature vortexing provided the maximum derivatization efficiency, while the reaction conditions had a little effect on the EF of (*R*)-alkaloids. Table 1**S** demonstrates that (*1S*)-(-)-camphanic chloride did not preferentially derivatize a particular enantiomer (i.e., chiral discrimination was not observed).

Table 1 lists the ANOVA results and model coefficient of BBD, which revealed that the *p*-value for each model was less than 0.0001. There is only a 0.01% chance that this value could occur due to noise. A lack of fit *p*-values of 0.3619, 0.9071 and 0.1390 indicate that the lack of fit is not significantly associated to the pure error. Furthermore, the R^2 values for each model were 0.9901, 0.9784 and 0.9886. A higher R^2 indicates that the variability could be accounted for by the data satisfactorily fitting the model. Since the CV is standard deviation as a percentage of the mean, smaller values give better reproducibility. Each CV less than 10 indicated that the model was reproducible. All these statistical parameters show the reliability of this model. A multi-criteria decision analysis based on a desirability function was further applied to simultaneously optimize the conditions for all three analytes. The variables A, B, and C were set as "in range" from the −1 to +1 level. The goal for the RFF was set to "maximize", because the best derivatization efficiency was obtained with highest RRF. Therefore, a number of solutions were then produced using the Design Expert software and ranked according to their desirability. The solution with the highest desirability (0.950) was selected; the predicted RRF values for this solution were 0.875 (nornicotine), 1.166 (anatabine), and 0.133 (anabasine). The corresponding optimum conditions were 127.26 mg mL^{-1} (*1S*)-(-)-camphanic chloride, 21.01% (*w/w*) NaOH solution and reaction time of 38.52 min. For simplicity of operation, these values were rounded to 127 mg mL^{-1}, 21% *w/w*, and 39 min, respectively. The actual RFF values under the optimum conditions for derivatization were 0.867±0.018 (nornicotine), 1.192±0.039 (anatabine), and 0.130±0.005 (anabasine). These results indicates a good agreement between actual values and predicted values by the model, suggesting that the derivatization efficiency model of BBD was adequate.

3.3. Separation and identification of the camphanic derivatives

Baseline separation is critical for the accurate quantitation of chiral alkaloids. The t and R_S of the diastereomers and IS at different stationary phase, polarity and specification columns are listed in Table 2**S**. The results showed the performance of column Rtx 200 (60 *m* × 0.25 mm i.d. × 0.5 μm *df*) for the complete separation (R_s > 1.5) of three alkaloid enantiomers. Rtx-200 with a trifluoropropyl stationary phase often offer unique selectivity for electron-rich molecules with dipole-dipole interactions, due to their electrophilic nature of the fluorine-containing polymer [31].

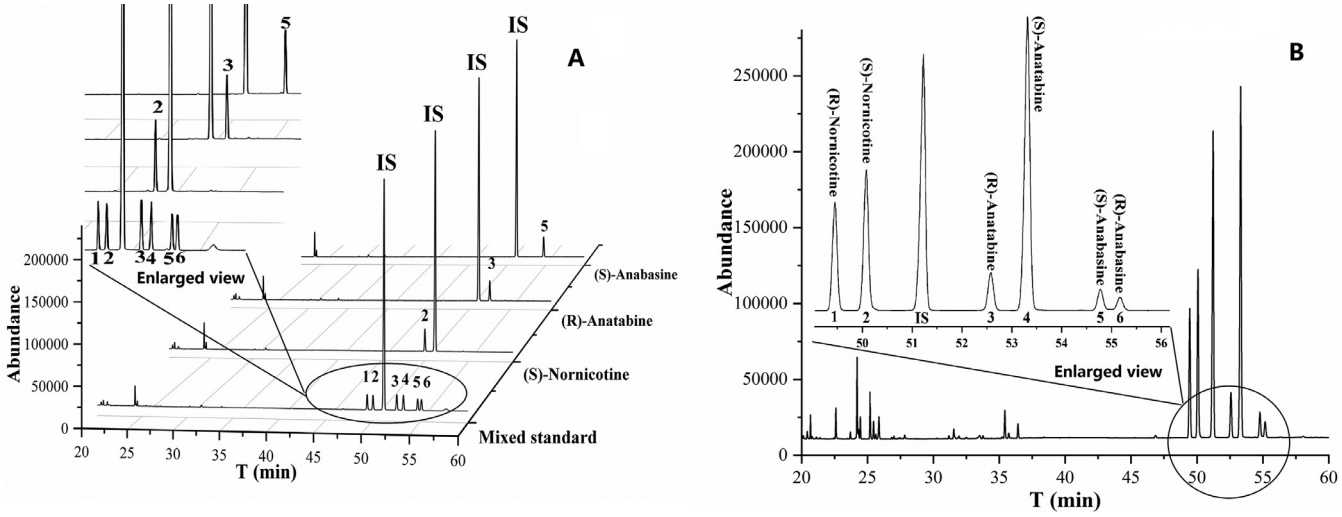

Fig. 2. Typical chromatographic profiles of the racemic standards, (*S*)-nornicotine, (*R*)-anatabine and (*S*)-anabasine **(A)** and FCT sample **(B)**. The detected compounds and number are listed in Table 2.

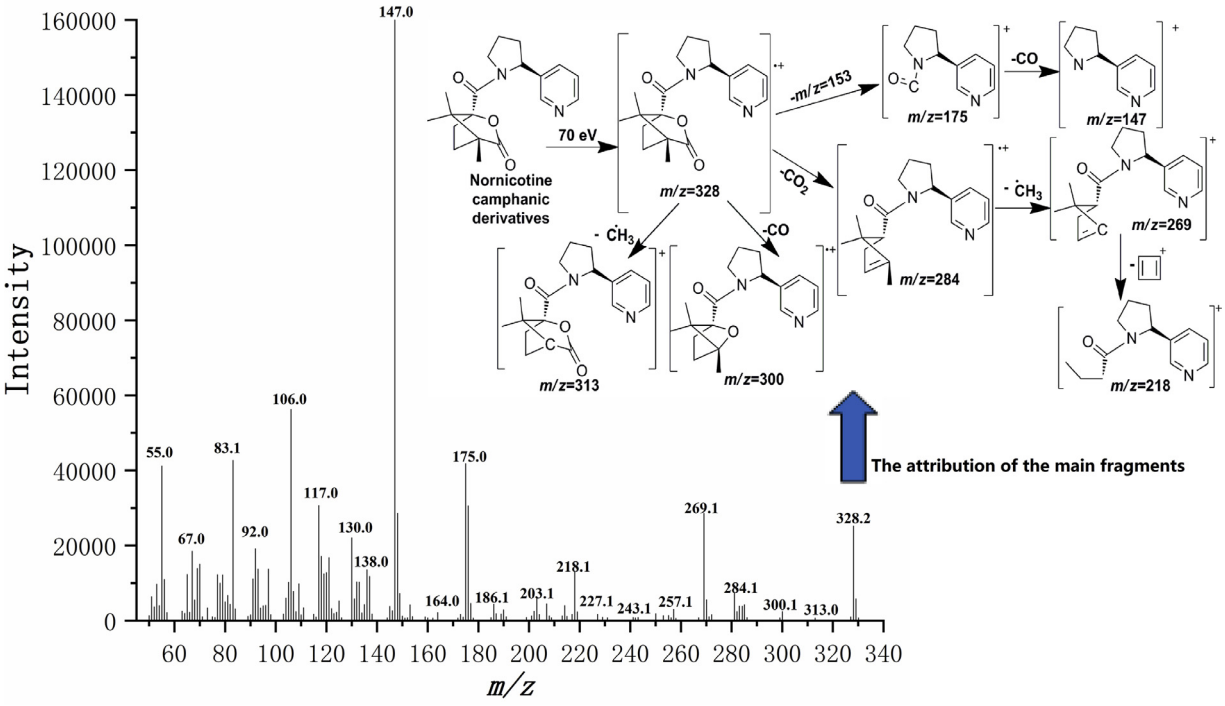

Fig. 3. The characteristic and attribution of the main fragment in the (*R*)-nornicotine camphanic derivative.

Furthermore, because this moderately polar column has a stably bonded stationary phase and resistance to temperatures as high as 330 °C, the R_s and peak shape show better stability over many thousands of injections. Typical chromatographic profiles of the racemic standards, (*S*)-nornicotine, (*R*)-anatabine and (*S*)-anabasine are shown in Fig. 2A.

The structures of the camphanic derivatives were confirmed by GC–MS. To the best of our knowledge, the mass spectra of these compounds have not been reported before. The attribution of the main fragment in the (*R*)-nornicotine camphanic derivative is presented in Fig. 3 and the characteristics of the mass spectra of the other camphanic derivatives are shown in Fig. 1S. These camphanic derivatives showed a similar fragmentation behavior. Taking nornicotine as an example, the molecular ion peaks (M) at m/z = 328 was present with medium intensity. The main characteristic ions were m/z = 175 and 147, which represented a loss of m/z = 153 **[**4,7,7-trimethyl-2-oxabicyclo[2.2.1] heptan-3-one**]**$^{\cdot+}$ from M, and the subsequent loss of m/z = 28 (neutral carbon monoxide). The ion with m/z = [M-153–28] was the base peak (BP) with the highest abundance. The lower abundance ions at m/z = 313, 300 and 284 represent the loss of a methyl radical [M-15], carbon monoxide [M-28] and carbon dioxide [M-44]. The other higher abundance ion with m/z = 269 and 218 were derived from the further loss of a methyl radical [M-44–15] and [C4H3]$^{\cdot+}$ ion [M-44–15–51]. The ions with m/z values below 147 represent a mixture of [nornicotine]$^{\cdot+}$ and **[**4, 7, 7-trimethyl-2-oxabicyclo[2.2.1] heptan-3-one**]**$^{\cdot+}$ fragments and most had medium intensity. The knowledge of the fragmentation mechanisms obtained from this study could potentially be used to identify the structure of primary or secondary amines alkaloids that have no available authentic standards but have similar chemical structures to known alkaloids.

Table 2
Calibration curve and ME parameters, LOD and LOQ values in four tobacco matrices.

Compounds/No	Matrix type	Standard curve	R^2	Normality test/p value	ME/%	LOD/μg g^{-1}	LOQ/μg g^{-1}
(*R*)- nornicotine/1	S	$y = 1.671x-0.0004256$	0.9995	0.324	_	_	_
	FCT	$y = 1.735x-0.0003249$	0.9992	0.683	3.83	0.087	0.29
	BT	$y = 1.706x-0.0003966$	0.9995	0.595	2.09	0.087	0.29
	OT	$y = 1.745x-0.0003419$	0.9992	0.905	4.43	0.087	0.29
	FD-FFCT	$y = 1.712x-0.0004615$	0.9990	0.787	2.45	0.17	0.59
(*S*)-nornicotine/2	S	$y = 1.669x-0.0004226$	0.9996	0.332	_	_	_
	FCT	$y = 1.726x-0.0005092$	0.9991	0.546	3.42	0.091	0.30
	BT	$y = 1.695x-0.0004407$	0.9994	0.626	1.56	0.091	0.30
	OT	$y = 1.753x-0.0002638$	0.9989	0.719	5.03	0.092	0.31
	FD-FFCT	$y = 1.718x-0.0004511$	0.9989	0.846	2.94	0.18	0.61
(*R*)-anatabine/3	S	$y = 1.481x+0.0003451$	0.9998	0.363	_	_	_
	FCT	$y = 1.533x+0.0005509$	0.9993	0.0700	3.51	0.11	0.37
	BT	$y = 1.529x+0.0004594$	0.9992	0.100	3.24	0.11	0.37
	OT	$y = 1.535x+0.0001740$	0.9991	0.981	3.65	0.11	0.37
	FD-FFCT	$y = 1.511x+0.0002004$	0.9998	0.0573	2.03	0.22	0.73
(*S*)-anatabine/4	S	$y = 1.479x+0.0001944$	0.9999	0.134	_	_	_
	FCT	$y = 1.523x+0.0002134$	0.9990	0.509	2.95	0.11	0.37
	BT	$y = 1.509x+0.0002669$	0.9995	0.170	2.01	0.12	0.39
	OT	$y = 1.565x+0.0001593$	0.9996	0.632	5.79	0.12	0.39
	FD-FFCT	$y = 1.524x+0.0002234$	0.9996	0.235	3.02	0.23	0.76
(*S*)-anabasine/5	S	$y = 1.444x-0.0007795$	0.9995	0.193	_	_	_
	FCT	$y = 1.516x-0.0005245$	0.9993	0.926	4.99	0.12	0.40
	BT	$y = 1.497x-0.0007699$	0.9994	0.477	2.98	0.12	0.40
	OT	$y = 1.543x-0.0005531$	0.9992	0.854	6.86	0.11	0.38
	FD-FFCT	$y = 1.506x-0.0005355$	0.9994	0.934	4.29	0.24	0.81
(*R*)-anabasine/6	S	$y = 1.440x-0.0008278$	0.9997	0.196	_	_	_
	FCT	$y = 1.498x-0.0007685$	0.9992	0.530	4.03	0.12	0.40
	BT	$y = 1.492x-0.0007461$	0.9993	0.531	3.61	0.12	0.40
	OT	$y = 1.555x-0.0004738$	0.9994	0.840	7.99	0.11	0.38
	FD-FFCT	$y = 1.493x-0.0006164$	0.9995	0.962	3.68	0.24	0.81

3.4. Evaluation of the linearity, matrix effect, and limits of detection and quantitation

The linear regression and ME parameters, LOD and LOQ values in four tobacco matrices are listed in Table 2 and Fig. 2S. R^2 values for all curves were greater than 0.9989, with most above 0.9990. The statistical normality test ($p > 0.05$) for each curve indicated a normal distribution of the residuals, further demonstrating that the linear model was satisfactory. ME can result in signal suppression or enhancement due to the co-extraction of matrix components affecting the derivatization efficiency or injection active sites [32]. The results showed that the ME (%) of each enantiomer was between 1.56% and 7.99% in the four matrices. The ME was positive for all compounds, indicating a slight enhancement of the signal. The ME usually results in an enhancement of the analyte signal in GC, as the co-extracted matrix components can occupy some of the available sites in the liner, resulting in the transfer of a greater amount of the analyte to the chromatographic column [33]. These results indicated that the solvent matched-calibration curve could be used to quantify real samples with errors in their quantification below 10%. When the sample concentration exceeds the linear range, the dilution with methyl tert–butyl ether were used before GC injection. The LODs and LOQs ranged from 0.087 to 0.24 μg g^{-1} and 0.29 to 0.81 μg g^{-1}, respectively. Because the sample weight for FD-FFCT was half that of the other samples, its LODs and LOQs were doubled.

3.5. Evaluation of the recovery, precision and storage stability

The mean recoveries for all analytes in four tobacco matrices ranged from 94.3% to 104.2%. According to the calculation of solvent-matched standard curves, the total concentrations of each analyte ((*R*)-nornicotine + (*S*)-nornicotine, (*R*)-anatabine + (*S*)-anatabine, and (*R*)-anabasine + (*S*)-anabasine: 756.2 ± 9.5, 1282.1 ± 12.8 and 136.0 ± 3.6 μg g^{-1}, respectively) in the standard reference sample using the proposed method were compared. The results showed that there was no significant difference. The precision expressed as the RSD_R ranged from 0.51% to 3.89%, depending on the spiked analyte and the matrix. The HorRat values in the present study were between 0.15 and 0.65. Few of the HorRat values were less than 0.3 in this method, due to the selection of an appropriate internal standard compound and the good stability of the derivatives. The storage stability over 7 d at room temperature was very good, with RDs between 0.63% and 3.58%. These results indicated that this method was sufficiently accurate and precise to permit reliable enantiomeric profiling of alkaloids in different tobacco matrices (Table 3).

3.6. Comparison of the validated method with other methods

The validated method was compared with other methods [11–13,15,21] in Table 3S. The chiral derivatization reagent (*1S*)-(-)-camphanic chloride is relatively common and inexpensive, and the derivatization reactions were completed by simply adding NaOH solution as a catalyst and applying room temperature vortexing for 39 min. More importantly, the camphanic derivatives were completely separated using a simple and stable achiral column. Using the structural analog of 4-phenylpiperidine as an internal standard, the optimized method provided strict quantitative data and exhibited a simple sample pretreatment, wide linear range, excellent accuracy, outstanding precision, minimal ME, and high stability.

3.7. Changes in the concentration and enantiomeric profiling of the alkaloids in cultivars

FCT cultivars with different genetic backgrounds are an important inherent factor that affects the composition of alkaloid

Table 3
Recovery, precision and stability study in four tobacco matrices.

Compounds	Matrix types	Spiked concentration/$\mu g\ g^{-1}$		Recovery/%		Precision				Stability/%
		L[a]	H[a]	L	H	RSD_R L/%	RSD_R H/%	HorRat L	HorRat H	
(*R*)- nornicotine	FCT	200	400	96.4	97.3	0.61	1.55	0.15	0.39	1.56
	BT	300	600	96.0	99.0	1.05	1.61	0.26	0.54	1.38
	OT	100	200	95.2	99.6	1.89	2.55	0.47	0.64	1.89
	FD-FFCT	250	500	94.4	96.9	0.98	1.45	0.25	0.48	1.78
(*S*)- nornicotine	FCT	200	400	96.1	97.8	0.73	1.35	0.18	0.34	1.87
	BT	300	600	95.7	98.6	0.89	1.51	0.30	0.50	1.76
	OT	100	200	94.3	98.6	1.34	1.87	0.34	0.47	2.01
	FD-FFCT	250	500	95.6	97.1	1.04	1.15	0.26	0.29	1.99
(*R*)- anatabine	FCT	500	1000	97.6	99.2	1.34	0.57	0.34	0.19	0.63
	BT	500	1000	96.8	99.1	0.89	1.35	0.22	0.45	0.78
	OT	50	100	97.9	98.7	2.65	2.08	0.44	0.52	1.45
	FD-FFCT	400	800	97.7	99.3	1.43	0.78	0.36	0.20	0.86
(*S*)- anatabine	FCT	500	1000	98.1	99.5	1.00	0.62	0.33	0.21	0.55
	BT	500	1000	98.3	98.7	0.54	0.96	0.18	0.32	0.81
	OT	50	100	97.3	98.4	1.18	0.78	0.30	0.20	1.34
	FD-FFCT	400	800	98.3	99.2	1.56	0.51	0.52	0.17	0.77
(*S*)- anabasine	FCT	40	80	98.4	99.5	2.31	1.71	0.58	0.43	2.11
	BT	50	100	95.7	96.6	1.83	1.15	0.46	0.29	1.89
	OT	5	10	102.1	103.2	3.65	2.98	0.61	0.50	3.12
	FD-FFCT	50	100	96.1	97.6	1.94	1.12	0.49	0.28	2.45
(*R*)- anabasine	FCT	40	80	98.7	101.3	1.98	1.25	0.33	0.31	2.52
	BT	50	100	96.1	97.9	2.17	1.29	0.54	0.32	2.24
	OT	5	10	104.2	99.7	3.89	3.06	0.65	0.51	3.58
	FD-FFCT	50	100	95.9	97.3	1.67	0.89	0.42	0.22	2.79

[a] L and H represent spiked concentration with low- and high-levels.

Table 4
Concentrations and enantiomeric profiling of alkaloids in seven cultivars.

Cultivar	Concentration[a]				EF (*R*)-enantiomer		
	Nicotine/mg g^{-1}	Nornicotine/$\mu g\ g^{-1}$	Anatabine/$\mu g\ g^{-1}$	Anabasine/$\mu g\ g^{-1}$	Nornicotine/%	Anatabine/%	Anabasine/%
NC297	34.2 ± 3.0	841 (2.5%)±77.8	1189 (3.5%)±100.5	187(0.55%)±14.6	54.2 ± 2.2	14.2 ± 0.63	43.8 ± 0.5
Bina1	35.3 ± 3.1	900 (2.6%)±83.0	1489 (4.2%)±165.6	222 (0.63%)±14.4	49.6 ± 2.5	15.3 ± 0.58	43.2 ± 0.7
K326	39.0 ± 3.7	1205(3.1%)±124.0	1835(4.7%)±170.3	258 (0.66%)±23.2	47.0 ± 1.6	14.9 ± 0.75	44.2 ± 0.8
Corker17	44.1 ± 4.6	1450(3.3%)±133.1	1497 (3.4%)±125.6	229(0.52%)±17.8	51.2 ± 1.7	16.2 ± 0.87	45.3 ± 0.7
NC82	46.5 ± 5.4	3220(6.9%)±359.0	3049(6.6%)±279.3	290 (0.63%)±23.6	24.1 ± 1.1	15.2 ± 0.90	44.4 ± 1.2
NCTG55	54.5 ± 3.9	6182(11.3%)±539.0	1927(3.5%)±154.7	223 (0.41%)±15.6	13.7 ± 0.5	14.6 ± 0.60	45.0 ± 0.5
NC95	56.2 ± 5.2	1454(2.6%)±139.7	2568(4.6%)±205.2	281(0.50%)±21.5	55.7 ± 2.0	14.4 ± 0.58	45.7 ± 1.0
	Difference analysis among the seven cultivars						
Fold change	1.6	7.3	2.6	1.6	4.1	1.1	1.1
RSD	19.8%	89.0%	34.0%	15.1%	38.9%	4.5%	2.0%

[a] Data presented as mean(percentage ratio with nicotine)±SD for six replicates.

metabolites [34]. In this study, we investigated the concentrations and enantiomeric profiling of nornicotine, anatabine, and anabasine in FCT from seven cultivars with different nicotine synthesis levels (low, medium, and high). The chromatographic profile of a typical FCT sample is shown in Fig. 2B. The nicotine concentration was analyzed using a previously reported method [1]. As shown in Table 4, nicotine was the predominant alkaloid in all seven cultivars. Large coefficients of variation, being 19.8%, 89.0%, 34.0%, 15.1%, and 38.9%, were found for the concentrations of nicotine, nornicotine, anatabine, anabasine, and the EF of (*R*)-nornicotine, respectively. The changes in the maximum value were more than 1.5 times the minimum values. However, the cultivar had little influence on the EFs of (*R*)-anatabine and (*R*)-anabasine in the FCT. Generally, cultivars with higher nicotine concentrations showed higher nornicotine concentrations, except in the case of NC95. This result can be attributed to the fact that nornicotine is mainly, if not exclusively, synthesized through the *N'*-demethylation of nicotine by nicotine demethylases, which belong to the CYP82E subfamily of cytochrome P450 monooxygenases, while the precursors of anatabine and anabasine are not derived from nicotine [35]. Nornicotine is one most abundant minor alkaloids, typically accounting for about 3% of the nicotine of FCT [36]. However, in NC82 and NCTG55 its concentration were 6.9% and 11.3%, respectively. Furthermore, NC82 and NCTG55 exhibited lower EF of (*R*)-nornicotine, at 24.1% and 13.7%, respectively. This may have been due to high expression of the CYP82E4 nicotine demethylase gene or a CYP82E4-like gene, which would decrease the EF of (*R*)-nornicotine during senescence or the curing processes, as these genes result in a higher preference for (*S*)-nicotine than CYP82E5v2 and CYP82E10 [21]. Nicotine demethylase specifically produces high concentrations of (*S*)-nornicotine from (*S*)-nicotine [37]. Because nornicotine contributes to undesirable smoke quality and the harmful smoke constituent NNN may be nornicotine derived, researchers are trying to discover and breed new cultivars with genotypes that reduce nornicotine levels with lower expression of nicotine demethylation genes, especially CYP82E4 or CYP82E4-like genes, in the leaf [38]. Thus, we confirmed that the cultivar of FCT had a significant impact on its nornicotine, anatabine, and anabasine concentrations and EF of (*R*)-nornicotine.

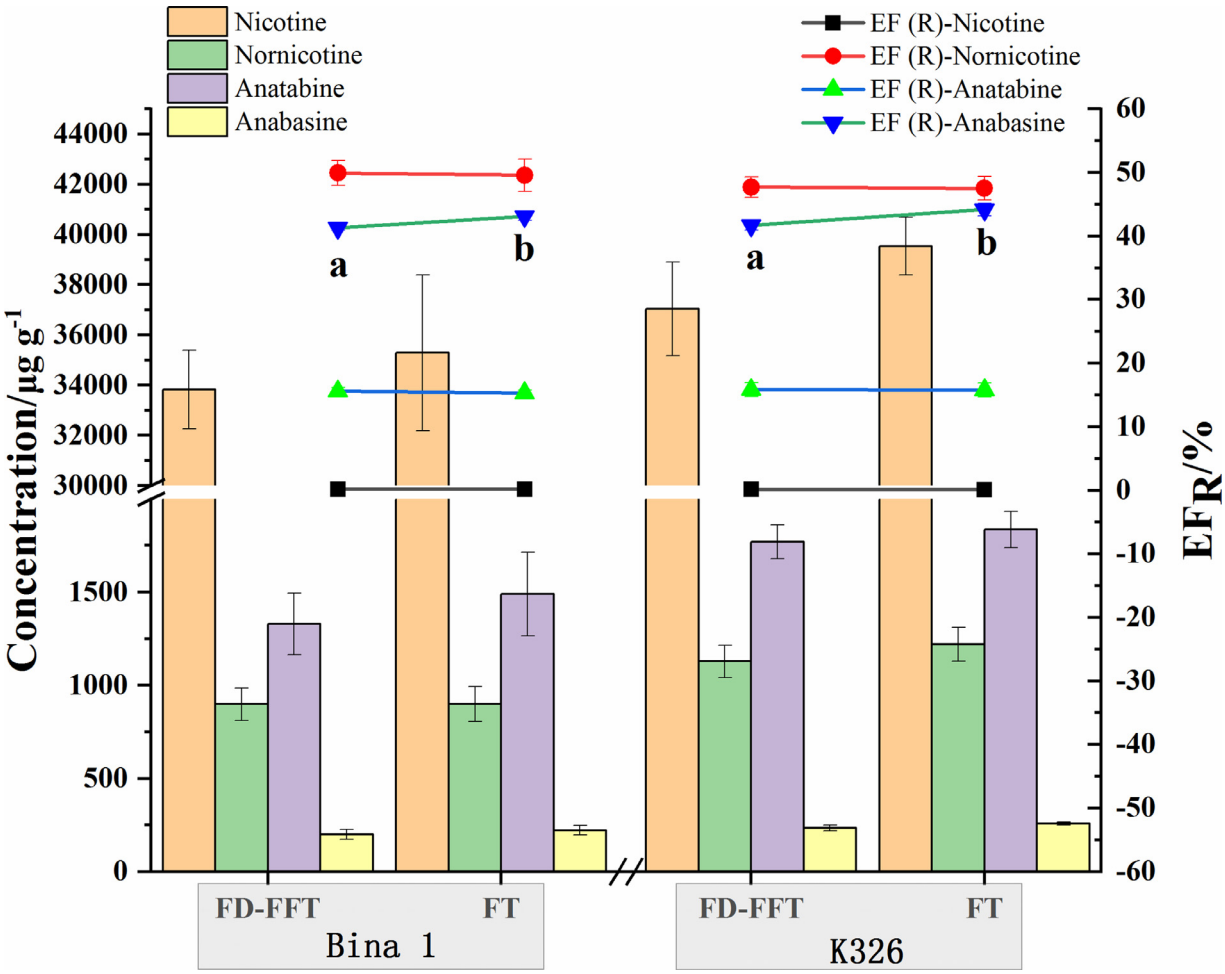

Fig. 4. Effects of curing processes on the concentrations and enantiomeric profiling of the alkaloids in Bina1 and K326 (significant differences were marked with different letters in EF of (*R*)-anabasine) (Fig. 4 print in color).

3.8. Effect of curing on the concentration and enantiomeric profiling of the alkaloids

To determine the changes in the alkaloid metabolite composition during the curing processes, we analyzed the concentrations and enantiomeric profiling of nornicotine, anatabine, and anabasine in FD-FFCT and FCT from Bina1 and K326. The nicotine concentration and EF were analyzed using our unpublished in-house method. Fig. 4 shows the effect of curing processes on the concentrations and enantiomeric profiling of the alkaloid. The concentrations of nicotine, nornicotine, anatabine and anabasine slightly but not significantly increased after curing, while previously published reports indicated that the concentrations of these alkaloids were relatively unchanged after curing [39]. This was attributed to the differences in dry-matter composition and dry-matter loss between FD-FFCT and FCT. The EF of (*R*)-nicotine, (*R*)-nornicotine, and (*R*)-anatabine also showed little change. These results showed no sign of demethylase activity in leaf tissue in Bina1 and K326, which is consistent with the fact CYP82E genes usually expressed only in root tissue for FCT [40]. Furthermore, the EF of (*R*)-anabasine showed a statistically significant increase, which is an interesting phenomenon. To further verify the effect of curing on the concentration and enantiomeric profiling of alkaloids, more cultivars with different genotypes should be investigated.

4. Conclusions

This study presents an improved camphanic chloride derivatization and achiral GC–NPD method for the quantitation of enantiomers of nornicotine, anatabine, and anabasine in tobacco. These alkaloids were completely separated using an achiral column with a trifluoropropyl stationary phase. The method was fully validated using four tobacco matrices, and was found to have excellent performance, with a wide linear range, excellent accuracy, outstanding precision and minimal ME. The method was successfully applied to analyze the enantiomeric profiling of FCT cultivars and curing processes, which revealed that the tobacco cultivar had a significant impact on the nornicotine, anatabine, anabasine concentration and EF of (*R*)-nornicotine, whereas the only a significant change induced by the curing processes was an increase in the EF of (*R*)-anabasine. Furthermore, this method could also enable the tentative screening and identification of unknown alkaloids of primary or secondary amines in other matrices.

Declaration of Competing Interest

The authors declare that they have no known competing financial interests or personal relationships that could have appeared to influence the work reported in this paper.

CRediT authorship contribution statement

Kai Cai: Conceptualization, Methodology, Data curation, Writing - original draft. **Huina Zhao:** Data curation, Writing - original draft. **Runsheng Yin:** Writing - review & editing. **Yechun Lin:** Methodology, Investigation. **Bo Lei:** Methodology, Investigation. **Anping Wang:** Visualization, Investigation. **Wenjie Pan:** Software, Validation. **Bin Cai:** Visualization, Investigation. **Weichang Gao:** Supervision, Conceptualization, Project administration. **Feng Wang:** Supervision, Conceptualization, Project administration.

Acknowledgements

This work was supported by Science and Technology Program of Science and Technology Department of Guizhou Province (No. 20191212, 20182335), the Program of Guizhou Academy of Tobacco Science (No. GZYKS2019–04), the Talent Project of Science and Technology Department of Guizhou Province (No. 20206020) and the Program of Guizhou Provincial Tobacco Company (No. 201910, 201722, 201706).

Supplementary materials

Supplementary material associated with this article can be found, in the online version, at doi:10.1016/j.chroma.2020.461361.

References

[1] K. Cai, Z.M. Xiang, J. Zhang, S.P. Zhou, Y.G. Feng, Z.L. Geng, Determination of eight tobacco alkaloids in flue-cured tobacco samples by gas chromatography with nitrogen chemiluminescence detection (NCD), Anal. Methods 4 (2012) 2095–2100, doi:10.1039/C2AY25067E.
[2] E. Konstantinou, F. Fotopoulou, A. Drosos, N. Dimakopoulou, Z. Zagoriti, A. Niarchos, D. Makrynioti, D. Kouretas, K. Farsalinos, G. Lagoumintzis, K. Poulas, Tobacco-specific nitrosamines: a literature review, Food Chem. Toxicol. 118 (2018) 198–203, doi:10.1016/j.fct.2018.05.008.
[3] G. Hellinghausen, D. Roy, Y. Wang, J.T. Lee, D.A. Lopez, C.A. Weatherly, D.W. Armstrong, A comprehensive methodology for the chiral separation of 40 tobacco alkaloids and their carcinogenic *E/Z*-(*R, S*)-tobacco-specific nitrosamine metabolites, Talanta 181 (2018) 132–141, doi:10.1016/j.talanta.2017.12.060.
[4] B. Cai, B. Siminszky, J. Chappell, R.E. Dewey, L.P. Bush, Enantioselective demethylation of nicotine as a mechanism for variable nornicotine composition in tobacco leaf, J. Biol. Chem. 287 (2012) 42804–42811, doi:10.1074/jbc.m112.413807.
[5] J.C. Shen, X.G. Shao, Determination of tobacco alkaloids by gas chromatography-mass spectrometry using cloud point extraction as a preconcentration step, Anal. Chim. Acta 561 (2006) 83–87, doi:10.1016/j.aca.2006.01.002.
[6] Y. Li, T. Pang, J.L. Shi, X.P. Lu, J.H. Deng, Q. Lin, Simultaneous determination of alkaloids and their related tobacco-specific nitrosamines in tobacco leaves using LC-MS-MS, J Chromatogr. Sci. 53 (2015) 1730–1736, doi:10.1093/chromsci/bmv082.
[7] J.R. Shifflett, L. Watson, D.J. McNally, D.Z. Bezabeh, Simultaneous determination of tobacco alkaloids, tobacco-specific nitrosamines, and solanesol in consumer products using UPLC-ESI-MS/MS, Chromatographia 81 (2018) 517–523, doi:10.1007/s10337-017-3462-4.
[8] R.C. Moldovan, E. Bodoki, A.C. Servais, J. Crommen, R. Oprean, M. Fillet, (+) or (−)-1-(9-fluorenyl)ethyl chloroformate as chiral derivatizing agent: a review, J. Chromatogr. A 1513 (2017) 1–17, doi:10.1016/j.chroma.2017.07.045.
[9] G. Alvarez-Rivera, M. Bueno, D. Ballesteros-Vivas, A. Cifuentes, Chiral analysis in food science, Trac-Trend Anal. Chem. 123 (2019) 115761, doi:10.1016/j.trac.2019.115761.
[10] S.M. Xie, X.X. Chen, J.H. Zhang, L.M. Yuan, Gas chromatographic separation of enantiomers on novel chiral stationary phases, Trac-Trend Anal. Chem. 124 (2020) 115808, doi:10.1016/j.trac.2020.115808.
[11] D.W. Armstrong, X.D. Wang, J.T. Lee, Y.S. Liu, Enantiomeric composition of nornicotine, anatabine, and anabasine in tobacco, Chirality 11 (1999) 82–84 10.1002/(SICI)1520-636X(1999)11:1<82::AID−CHIR14>3.0.CO;2-C.
[12] B.Z. Liu, C.Y. Chen, D. Wu, Q.D. Su, Enantiomeric analysis of anatabine, nornicotine and anabasine in commercial tobacco by multi-dimensional gas chromatography and mass spectrometry, J. Chromatogr. B 865 (2008) 13–17, doi:10.1016/j.jchromb.2008.01.034.
[13] H.H. Ji, Y. Wu, F. Fannin, L. Bush, Determination of tobacco alkaloid enantiomers using reversed phase UPLC/MS/MS, Heliyon 5 (2019) e01719, doi:10.1016/j.heliyon.2019.e01719.
[14] S.Q. Tong, H. Zhang, M.M. Shen, Y. Ito, J.Z. Yan, Enantioseparation of mandelic acid derivatives by high performance liquid chromatography with substituted β;-cyclodextrin as chiral mobile phase additive and evaluation of inclusion complex formation, J. Chromatogr. B 962 (2014) 44–51, doi:10.1016/j.jchromb.2014.05.026.
[15] S. Kodama, A. Morikawa, K. Nakagomi, A. Yamamoto, A. Sato, K. Suzuki, T. Yamashita, T. Kemmei, A. Taga, Enantioseparation of nicotine alkaloids in cigarettes by CE using sulfated β;-CD as a chiral selector and a capillary coated with amino groups, Electrophoresis 30 (2009) 349–356, doi:10.1002/elps.200800340.
[16] M.N. Newmeyer, M. Concheiro, M.A. Huestis, Rapid quantitative chiral amphetamines liquid chromatography-tandem mass spectrometry: method in plasma and oral fluid with a cost-effective chiral derivatizing reagent, J. Chromatogr. A 1358 (2014) 68–74, doi:10.1016/j.chroma.2014.06.096.
[17] M. Okada, A. Yamamoto, S. Aizawa, A. Taga, H. Terashima, S. Kodama, HPLC separation of sulforaphane enantiomers in broccoli and its sprouts by transformation into diastereoisomers using derivatization with (*S*)-leucine, J. Agric. Food Chem. 65 (2017) 244–250, doi:10.1021/acs.jafc.6b04966.
[18] Z. Wang, Schotten-Baumann reaction (Schotten-Baumann acylation), Compr. Org. Name React. Reag. 573 (2010) 2536–2539, doi:10.1002/9780470638859.conrr573.
[19] H. Licea-Perez, S. Wang, C. Rodgers, C.L. Bowen, K. Fang, M. Szapacs, C.A. Evans, Camphanic acid chloride: a powerful derivatization reagent for stereoisomeric separation and its DMPK applications, Bioanalysis 7 (2015) 3005–3017, doi:10.4155/bio.15.219.
[20] P. Jacob III, N.L. Benowitz, A.T. Shulgin, Synthesis of optically pure deuterium-labelled nicotine, nornicotine and cotinine, J. Labelled Compd. Rad. 25 (1988) 1117–1128, doi:10.1002/jlcr.2580251009.
[21] B. Cai, L.P. Bush, Variable nornicotine enantiomeric composition caused by nicotine demethylase CYP82E4 in tobacco leaf, J. Agric. Food Chem. 60 (2012) 11586–11591, doi:10.1021/jf303681u.
[22] L. Chen, D.L. Capone, D.W. Jeffery, Chiral analysis of 3-sulfanylhexan-1-ol and 3-sulfanylhexyl acetate in wine by high-performance liquid chromatography-tandem mass spectrometry, Anal. Chim. Acta 998 (2018) 83–92, doi:10.1016/j.aca.2017.10.031.
[23] C.L. Ke, Q. Liu, L.D. Li, J.W. Chen, X.N. Wang, K. Huang, Simultaneous determination of eugenol, isoeugenol and methyleugenol in fish fillet using gas chromatography coupled to tandem mass spectrometry, J. Chromatogr. B 1031 (2016) 189–194, doi:10.1016/j.jchromb.2016.07.048.
[24] E. Rutkowska, B. Łozowicka, P. Kaczyński, Compensation of matrix effects in seed matrices followed by gas chromatography-tandem mass spectrometry analysis of pesticide residues, J. Chromatogr. A 1614 (2020) 460738, doi:10.1016/j.chroma.2019.460738.
[25] H. Dong, K.J. Xiao, Modified QuEChERS combined with ultra high performance liquid chromatography tandem mass spectrometry to determine seven biogenic amines in Chinese traditional condiment soy sauce, Food. Chem. 229 (2017) 502–508, doi:10.1016/j.foodchem.2017.02.120.
[26] L.L. Smith, B.Y. Liang, M.C. Booth, M.S. Filigenzi, A. Tkachenko, C.L. Gaskill, Development and validation of quantitative ultraperformance liquid chromatography–tandem mass spectrometry assay for anticoagulant rodenticides in liver, J. Agric. Food Chem. 65 (2017) 6682–6691, doi:10.1021/acs.jafc.7b02280.
[27] W. Horwitz, R. Albert, The Horwitz ratio (HorRat): a useful index of method performance with respect to precision, J. AOAC Int. 89 (2006) 1095–1109, doi:10.1093/jaoac/89.4.1095.
[28] K. Cai, W.C. Gao, Y. Yuan, C.C. Gao, H.N. Zhao, Y.C. Lin, W.J. Pan, B. Lei, An improved in *situ* acetylation with dispersive liquid-liquid microextraction followed by gas chromatography–mass spectrometry for the sensitive determination of phenols in mainstream tobacco smoke, J. Chromatogr. A. 1603 (2019) 401–406, doi:10.1016/j.chroma.2019.05.007.
[29] L. Ding, L.Q. Sheng, H.W. Tong, G.P. Yong, S.M. Liu, Determination of main alkaloid in tobacco by capillary gas chromatography with solvent extraction, Chin. J. Anal. Chem. 32 (2004) 1161–1164.
[30] D.H.B. Ripin, M. Vetelino, 2-Methyltetrahydrofuran as an alternative to dichloromethane in 2-phase reactions, Synlett 15 (2003) 2353, doi:10.1055/s-2003-42091.
[31] A.J. Jenkins, K.M. Sarconi, H.N. Raaf, Determination of olanzapine in a postmortem case, J. Anal. Toxicol. 22 (1998) 605–609, doi:10.1093/jat/22.7.605.
[32] M.M. Rahman, A.M.A. El-Aty, J.H. Shim, Matrix enhancement effect: a blessing or a curse for gas chromatography?—a review, Anal. Chim. Acta 801 (2013) 14–21, doi:10.1016/j.aca.2013.09.005.
[33] M. Murcia-Morales, V. Cutillas, A.R. Fernández-Alba, Supercritical fluid chromatography and gas chromatography coupled to tandem mass spectrometry for the analysis of pyrethroids in vegetable matrices: a comparative study, J. Agric. Food Chem. 67 (2019) 12626–12632, doi:10.1021/acs.jafc.9b00732.
[34] M. Banožić, J. Babić, S. Jokić, Recent advances in extraction of bioactive compounds from tobacco industrial waste—a review, Ind. Crops Prod. 144 (2020) 112009, doi:10.1016/j.indcrop.2019.112009.
[35] B. Cai, Enantioselective demethylation: the key to the nornicotine enantiomeric composition in tobacco leaf, (2012) https://uknowledge.uky.edu/pss_etds/5.
[36] P.X. Chen, N. Qian, H.R. Burton, S.C. Moldoveanu, Analysis of minor alkaloids in tobacco: a collaborative study, Beitr. Tabakforsch. Int. 21 (2005) 369–379, doi:10.2478/cttr-2013-0803.
[37] F. Mesnard, S. Girard, O. Fliniaux, R.K. Bhogal, F. Gillet, J. Lebreton, M.A. Fliniaux, R.J. Robins, Chiral specificity of the degradation of nicotine by *Nicotiana plumbaginifolia* cell suspension cultures, Plant Sci. 161 (2001) 1011–1018, doi:10.1016/S0168-9452(01)00509-X.
[38] R.S. Lewis, A.M. Jack, J.W. Morris, V.J.M. Robert, L.B. Gavilano, B. Siminszky, L.P. Bush, A.J. Hayes, R.E. Dewey, RNA interference (RNAi)-induced suppression

of nicotine demethylase activity reduces levels of a key carcinogen in cured tobacco leaves, Plant Biotechnol. J. 6 (2008) 346–354, doi:10.1111/j.1467-7652.2008.00324.x.

[39] Y. Abubakar, J.H. Young, W.H. Johnson, W.W. Weeks, Changes in moisture and chemical composition of flue-cured tobacco during curing, Tob. Sci. 44 (2000) 51–58, doi:10.3381/0082-4623-44.1.51.

[40] B. Cai, A.M. Jack, R.S. Lewis, R.E. Dewey, L.P. Bush, (*R*)-nicotine biosynthesis, metabolism and translocation in tobacco as determined by nicotine demethylase mutants, Phytochemistry 95 (2013) 188–196, doi:10.1016/j.phytochem.2013.06.012.